Stress relieved Zircaloy-4 recovery and recrystallization during fast anisothermal transients

Ahmed Chaieb, Nathanaël Mozzani, Antoine Ambard, Aurore Parrot, Alain Köster, Jérôme Crépin

Stress relieved Zircaloy-4 recovery and recrystallization during fast anisothermal transients

Ahmed Chaieb[a,b,*], Nathanaël Mozzani[a], Antoine Ambard[a], Aurore Parrot[a]

Alain Köster[b], Jérôme Crépin[b]

[a] *Département Matériaux et Mécanique des Composants*
EDF, Electricité de France, Avenue des Renardières, Ecuelles 77818, Moret-sur-Loing Cedex, France

[b] *Centre des Matériaux - Mines Paris- PSL Université, CNRS UMR 7633*
63 - 65 rue Henry Desbruères, BP 87, F-91003 Evry cedex, France

Highlights

- Kinetics of recovery recrystallization of fuel clads during transient heating.
- Cladding behaviour under anisothermal conditions.
- Tight competition between temperature and holding time.

Acknowledgements

The authors would like to thank operators who have contributed in the thermal cycle tests. Authors are grateful for their technical support and assistance. This work was funded by EDF through grant P117T.

Abstract

Cold-work stress-relieved Zircaloy-4 kinetics of recovery-recrystallization has been studied under dynamic conditions. A specific furnace dilatometer was used to heat Zircaloy-4 specimens up to $430\ °C \cdot s^{-1}$. Comparison of dynamic results with data of isothermal recovery and recrystallization showed that the process is delayed when the heating rate is increased. A model was proposed to describe the evolution of the material unrecrystallized fraction during rapid anisothermal transients. Comparisons showed a good agreement between the experimental results and the model predictions.

Keywords; recrystallization; recovery; RIA transients; anisothermal conditions; Zircaloy-4; reactivity initiated accident; fuel cladding

[*]Corresponding author. Email: ahmed-a.chaieb@edf.fr

1. Introduction

Zirconium alloys have been used as fuel cladding materials in nuclear reactors for several decades. Many studies were dedicated to the study of their behaviour during normal, incidental and accidental situations like RIA (Reactivity Initiated Accident) which is a design-basis accident to be accounted for in Pressurized Water Reactors (PWR) safety analysis. It is characterised by fast and complex thermo-mechanical transients that could potentially lead to the failure of the fuel rod cladding, i.e. the first containment barrier of radioactive products.
Macroscopic and expensive tests performed in experimental reactors such as CABRI [1], [2], [3] and NSRR [4], [5] permitted to characterize these transients: high strain rates (up to $5\ s^{-1}$), high heating rates (up to $1000\ °C \cdot s^{-1}$) and variable biaxial loading path.
Recrystallization studies are traditionally isothermal tests [6] [7] where specimens are held at target temperatures. The process of recovery-recrystallization depends on many parameters like temperature [6] [8] [9] [10] [11], annealing time [6] [9] [12] [13], chemical composition [6] [9] [14] [15] [16] and strain hardening [17]. The purpose of this study is to understand the effect of anisothermal transients on the recovery-recrystallization kinetics of unirradiated cold-work stress-relieved Zircaloy-4.
In order to determine the behaviour of fuel cladding materials, laboratory mechanical tests are carried out on cladding specimens. Almost all these tests, such as the ones from the PROMETRA database [18] are performed at constant temperature between 300 and 900°C. Depending on the test temperature, the material is either in the as-irradiated, annealed or recrystallized states. Understanding the kinetics of the transition from one state to the other is of prime interest when establishing a mechanical model relevant for transient conditions such as the RIA accident. As a first step of a larger research effort, this study deals with unirradiated material and the transition from the as-received state (cold-worked stress relieved) to the recrystallized state during anisothermal transients when the clad is not in thermal equilibrium and its temperature varies as function of the time.
As the study was carried out at a macroscopic scale, no distinction between strain hardening recovery and recrystallization was made. In fact, the evolution of mechanical properties is due to material recovery (annihilation of crystalline defects) which occurs without germination of new grains or to recrystallization which rebuilds the equilibrium state by germination and growth of new grains. Heating tests have been carried out at high heating rates, i.e. up to $430\ °C \cdot s^{-1}$ using an induction coil. The degree of recrystallization after each thermal transient was assessed via microhardness measurement. This method was used during previous studies [7] [8] [9] [10] [15] [19] [20] [21].
Experiments were therefore carried out to look for any difference in the recrystallization kinetics between rapid transients and long-time isothermal tests reported in the literature.

2. Experimental procedure

To determine the behavior of Zircaloy nuclear fuel cladding tubes during postulated fast temperature transients representative of RIA accident, this work was oriented to study the recrystallization which may occur in the range of heating rate [$25 - 430\ °C \cdot s^{-1}$].
A furnace dilatometer equipped with an induction coil (Figure 1) was used to heat a 10 mm length of unirradiated cold-worked and stress-relieved (CWSR) Zircaloy-4 tube specimens. A type-K thermocouple was welded in the specimen centre.

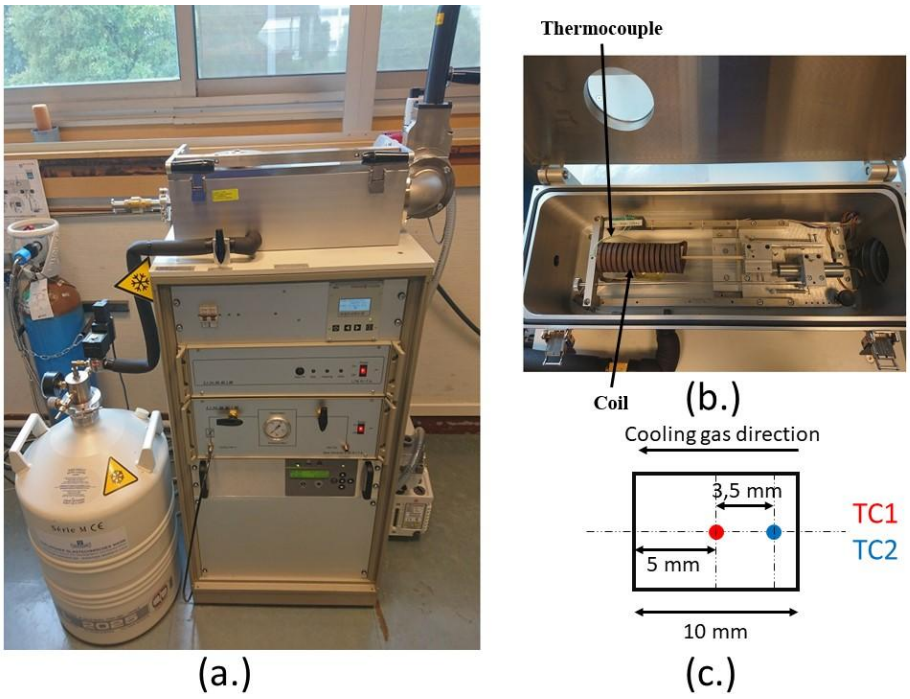

Figure 1. furnace (a.), furnace chamber (b.) and thermocouples positions (c.)

Alumina supports have been machined specifically to hold the specimens inside the coil. The system is controlled by the response of a thermocouple welded on the specimen regarding the heating sequence. The material is heated from room temperature to a target temperature at different heating rates. Once the target temperature has been reached, a gas (helium) is injected to rapidly cool the material. The quench was applied once the target peak temperature is reached, without any hold time. The test method is similar to the one described in [19]. It should be noted that the dilatometer is used as a furnace which allows fast heating rates. The furnace in the dilatometer was solely used. Specimens were heated in a primary vacuum to avoid material oxidation. A typical heating sequence is presented in Figure 2.

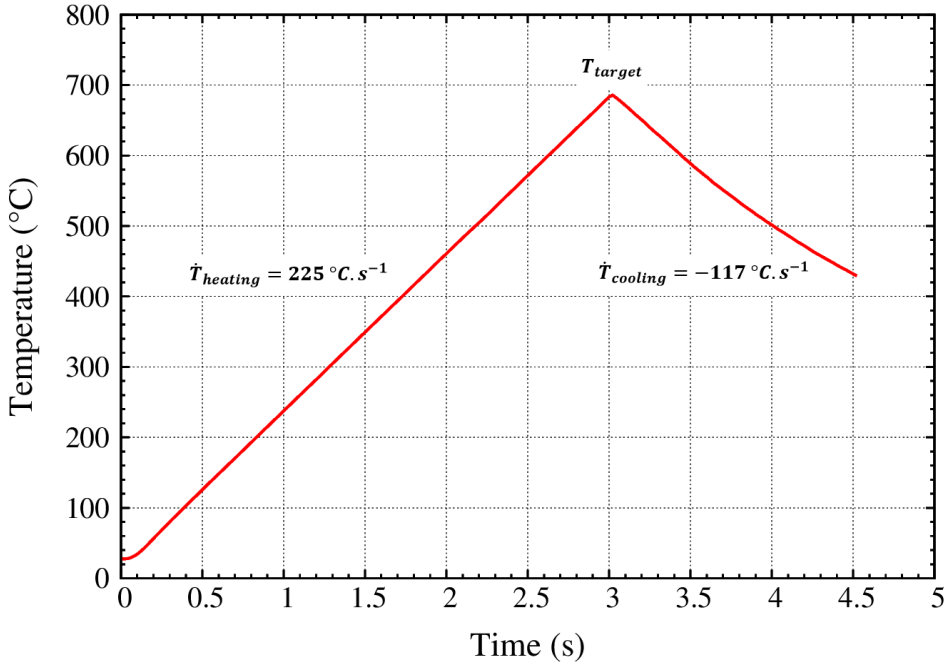

Figure 2. A typical heating sequence

Once the thermal cycle is carried out, the degree to which recrystallization had occurred in

each test was determined from Vickers microhardness measurements. The idea is to follow the same approach indicated in [19] in order to calculate, by Vickers microhardness (HV) measurements, a fraction of unrecrystallized material. Microhardness measurements were carried out using a 0.5 kg load.

In order to minimize the standard deviation, 20 microhardness measurements per sample were performed. For this reason, specimens were cut, then coated and polished up to the thermocouple location. Microhardness measurements were performed in the cross section corresponding to the thermocouple position in the specimen centre. The distance from the indentation centre to the edge of the sample must be greater than 2.5 x the diagonal of the indentation and the distance between two indentations must be greater than 3 x the length of the diagonal of one indentation.

There is a temperature gradient on the specimen which might affect the microhardness along the specimen. A study of axial temperature gradient was thus carried out. A first thermocouple was welded to the centre of the sample (x = 0 mm) and a second was welded at 3.5 mm from the centre (or 1.5 mm from the edge of the sample). Three heating rates were applied: $28, 225$ and $345\ °C \cdot s^{-1}$.

In Figure 3, these thermocouple measurements and the absolute value of the temperature difference are presented. At the onset of heating, the edge of the sample is slightly warmer. The temperature becomes then uniform over time. During the cooling period, the centre of the specimen is slightly warmer. This can be linked to the position of the second thermocouple (soldered to 3.5 mm from the centre) in relation to the cooling gas inlet position in the furnace enclosure. By comparing the difference of temperatures according to the applied heating rates, we notice that the temperature gradient becomes more important when the heating rate increases because the time for temperature homogenization is too short.

During the heating period, the maximum temperature difference is 13, 21 and 28 °C at heating rates of $28, 225$ and $345\ °C \cdot s^{-1}$ respectively. The highest discrepancies values were obtained “in the middle” of the heating and the cooling phase where conditions are the less stable. At peak temperature, the difference is lower than 13°C. Such a low difference is hardly detectable with microhardness. All measurement values can be treated as those obtained from the same heating conditions.

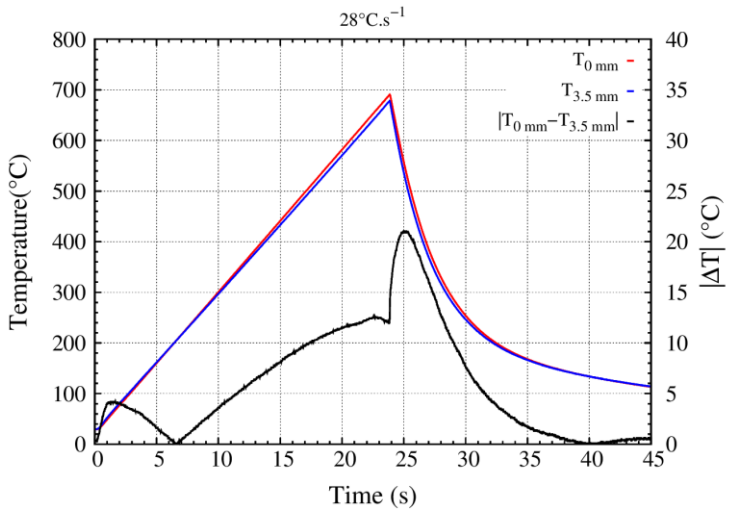

(a.)

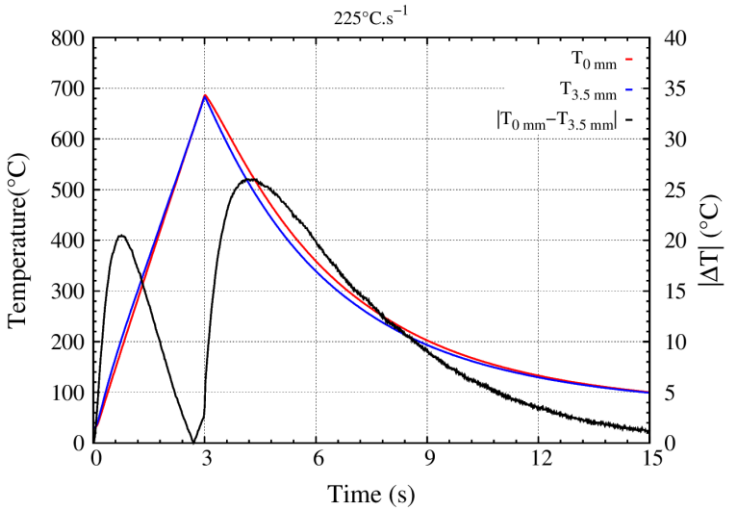

(b.)

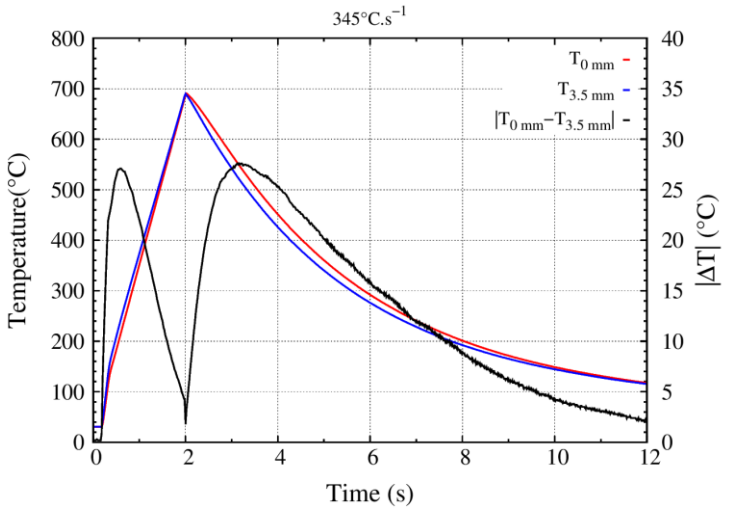

(c.)

Figure 3. Temperature difference at (a.) 28, (b.) 225 and (c.) 345 $°C \cdot s^{-1}$

3. Results and discussion

The different parameters of the thermal cycles applied are available in Table 1. For our tests, no holding time was applied when the maximum temperature is reached, cooling is directly triggered at this point. Our heating rates are calculated from the ambient temperature to the target (maximal) temperature. Cooling rates are calculated from the maximal temperature up to 430 °C. It was assumed that the recrystallization process is no longer active below this temperature.

The two reference states correspond to CWSR and completely recrystallized states. For the CWSR material, microhardness measurements are performed in the “as-received” state of the material which corresponds to a mean 228.791 HV with a standard deviation of 3.287 HV.

For the recrystallized state, a heat treatment was applied out at 830 °C for 20 minutes. The heating rate and the cooling rate are 1 and $-1\ °C \cdot s^{-1}$. Following this thermal cycle, a mean microhardness of 173.450 HV was calculated from measurements with a standard deviation of 2.476 HV.

Table 1. Thermal parameters of the heating sequences

Heating rate ($°C \cdot s^{-1}$)	Measured target temperature (°C)	Measured cooling rate ($°C \cdot s^{-1}$)	Measured unrecrystallized Fraction (-)
28	652.8	-204	0.980
	674.8	-134	0.818
	694.7	-137	0.428
	715.2	-130	0.336
	735	-141	0.133
	754.9	-135	0.061
225	685.6	-172	1.027
	705	-160	0.744
	723.8	-164	0.566
	745.1	-165	0.637
	739.2	-219	0.570
	763.4	-167	0.081
	764.6	-194	0.310
	784.7	-194	0.132
	784.5	-203	0.210
335	689.9	-159	1.087
	709.3	-183	0.839
	727.4	-176	0.670
	748.3	-188	0.607
	766.5	-182	0.258
	785.2	-154	0.186
	808.2	-185	0.135
430	693.6	-147	0.995
	713.4	-161	0.979
	731.9	-169	0.961
	741.4	-197	0.153
	771.4	-207	0.181
	776.8	-194	0.117
	791.8	-204	0.148

Table 2. Thermal parameters of the heating sequences adopted in Hunt's study [19]

Heating rate ($°C \cdot s^{-1}$)	Target temperature (°C)	Holding time (s)	Cooling rate ($°C \cdot s^{-1}$)
125	518	60	-220
	565	60	
	588	60	
	600	60	
	612	60	
	630	60	
	650	60	
	679	60	
	710	60	
0.5	570	--	-100
	596	--	
	604	--	
	617	--	
	628	--	
	637	--	
	642	--	
	654	--	
	666	--	
	691	--	
25	588	--	-130
	646	--	
	665	--	
	685	--	
	699	--	
	722	--	
	750	--	
	776	--	
	798	--	
	822	--	

These microhardness values of the CWSR and recrystallized materials correspond to fractions of unrecrystallized material of 1 and 0 respectively. The unrecrystallized material fraction F is calculated using Equation (1).

$$F = \frac{H_{measured} - H_{Rec}}{H_{CWSR} - H_{Rec}} = \frac{H_{measured} - 173.45}{228.79 - 173.45} \quad (1)$$

Firstly, several tests have been carried out at $28\ °C \cdot s^{-1}$ to compare our results with those of Hunt & Schulson [19]. Both studies yielded similar results at $25\ °C \cdot s^{-1}$ (Figure 4), thus confirming that the method is well reproduced because results of the two studies are comparable. Once all the microhardness measurements are carried out, the evolution of the fraction of the non-recrystallized material has been studied as a function of the maximum temperature reached during thermal cycle.

The results from the transient-heated specimens are shown in Figure 4. Error bars represent values inside of [$\overline{H}$- σ (H), $\overline{H}$+ σ (H)], i.e. 68 % of values. Error bars can extend to values of F greater than 1 or less than 0, that are not realistic.

Under isothermal conditions [19], with a holding time of 60 seconds, the recrystallization process start is detected between 526 and 576 °C and ends at 676 °C. As expected under

anisothermal conditions, recrystallization is dependent on the heating and cooling rates; the faster the heating rate, the higher is the starting recrystallization temperature. It seems that recrystallization starting temperature stabilizes at faster heating rates: Above $200\ °C \cdot s^{-1}$ the heating rate effect saturates. The temperature at which the transformation ends is also shifted to high temperatures with increasing heating rate. A metallurgical study would be interesting to identify the roles of recovery and recrystallization during these transients.

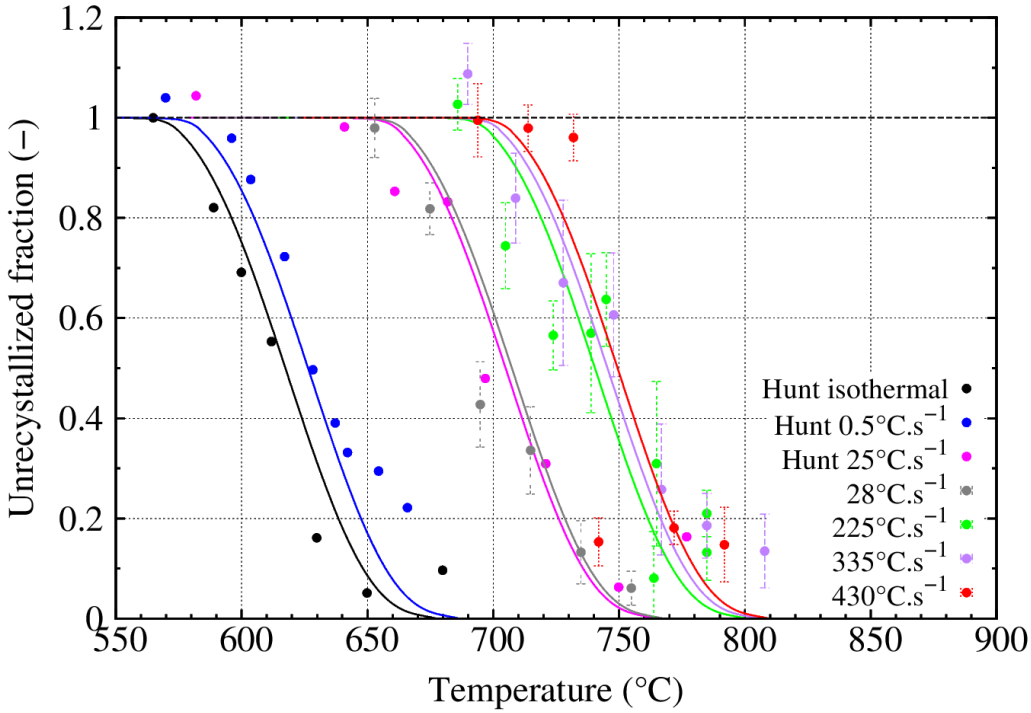

Figure 4. Recrystallization results from specimens heated up to $430\ °C.s^{-1}$ and model prediction

Many models were reported in literature to describe the recrystallization kinetics [7] [11] [15] [19] [20] [22] [23]. We were inspired from the study of Hunt & Schulson [19] at low heating rates to establish a model predicting the non-recrystallized fraction as a function of temperature, heating rate and holding time. Hunt's model was used in [13] to compare calculated recrystallization rates for unirradiated and irradiated Zircaloy at 550 and 650 °C.
The model proposed in [19] is given in Equation (2) (anisothermal or transient formulation) and Equation (3) (isothermal formulation).

$$\frac{dF}{dt} = -K.exp\left(-\frac{E}{RT}\right)F \tag{2}$$

$$F = F_0.exp\left(-K.t.exp\left(-\frac{E}{RT}\right)\right) \tag{3}$$

Where F is the fraction evolution of the non-recrystallized material depending on t, F_0 is the fraction of the initial non-recrystallized material, E is the activation energy for the recovery-recrystallization process, K is the Boltzmann's constant, t is the elapsed time, T is the absolute temperature in Kelvin and R is the gas constant ($R = 8.314\ J \cdot mol^{-1} \cdot K^{-1}$)
In this study Hunt's model [19] was adopted and extended to high heating rates by integrating a threshold temperature to describe the shift of recrystallization (Equation 4) to high temperature with increasing heating rate ($\dot{T} = dT/dt$).

$$T_{REC} = \alpha . \dot{T}^{\beta} \quad (4)$$

Where T_{REC} (K) is the starting temperature of recrystallization, α and β are model parameters such as: $\alpha = 849.37$ (K) and $\beta = 2492.32 \text{ x } 10^{-5}$ ($/\ln(\text{K} \cdot \text{s}^{-1})$). α and β parameters were identified on starting recrystallization temperatures obtained during anisothermal transients ($0.5, 25, 28, 225, 335$ and $430\ °C.s^{-1}$) using the least squares method.

$$F = \begin{cases} 1\ ;\ if\ T < T_{REC} \\ \dfrac{dF}{dt} = -K.exp\left(-\dfrac{E}{RT}\right)F\ ;\ if\ T \geq T_{REC} \end{cases} \quad (5)$$

The parameters K and E of the model are identified on the isothermal tests of Hunt [19] mentioned in Table 2 using Equation (3) and on the thermal transients at $0.5, 25, 28, 225, 335$ and $430\ °C \cdot s^{-1}$using Equation (5). The model parameters are given in Table 3.

Table 3. Model parameters for unrecrystallized material fraction

Study	K (-)	E (J.mol^{-1})	Validity
[19]	$2.08 \text{ x } 10^{18}$	345465.90	Isothermal + anisothermal up to $25\ °C \cdot s^{-1}$
This study	$1.87 \text{ x } 10^{18}$	344980.62	Isothermal + anisothermal up to $430\ °C \cdot s^{-1}$

There are no significant difference between the parameter of the annealing models fit on isothermal and slow transient and those fit of the fast ones. It shows that the main difference between fast and slow transient is just found in the starting recrystallization temperature. Once recrystallization starts, it proceeds with a fixed kinetic independent of the heating rate.
The microhardness measurements were determined on the samples after achievement of the cooling phase. At this stage, we cannot quantify the increment of the unrecrystallized fraction during cooling from maximal temperature to 430 °C at least. According to the model prediction presented in Equation (5), the actual value of the fraction of unrecrystallized material at the target or maximal temperature during the cycle is slightly higher than that estimated by the model at the end of the test (at room temperature). The mean value of the difference between the fraction of unrecrystallized material at peak temperature and the fraction of unrecrystallized material at the end of thermal cycle is presented in Table 4.

Table 4. Estimation of the decrease in the fraction of unrecrystallized material during the cooling phase

Heating rate ($°C \cdot s^{-1}$)	$\overline{F_{Tmax} - F_{25°C}}$
0.5	0
28	0.025
225	0.139
335	0.138
430	0.184

The model does not consider the microstructural evolutions during rapid transients. A further study at the microstructural scale would help to improve the model by describing the recovery and recrystallization processes.
In order to predict the metallurgical state of the material according to the experimental conditions, the model was used to evaluate the influence of the holding time before carrying out isothermal mechanical tests at a given temperature (tensile or creep isothermal tests for example). This allows us to evaluate the role of a potential metallurgical evolution. The model was applied to transients similar to those obtained in conventional furnace used for carrying out isothermal mechanical tests. In other words, the model was applied to temperature

sequences obtained following a heating at $15\ °C \cdot s^{-1}$ from ambient temperature to several target temperatures (which would be the temperatures of the isothermal tests). The fractions of the unrecrystallized material were estimated for several holding times. The obtained results are presented in Figure 5.

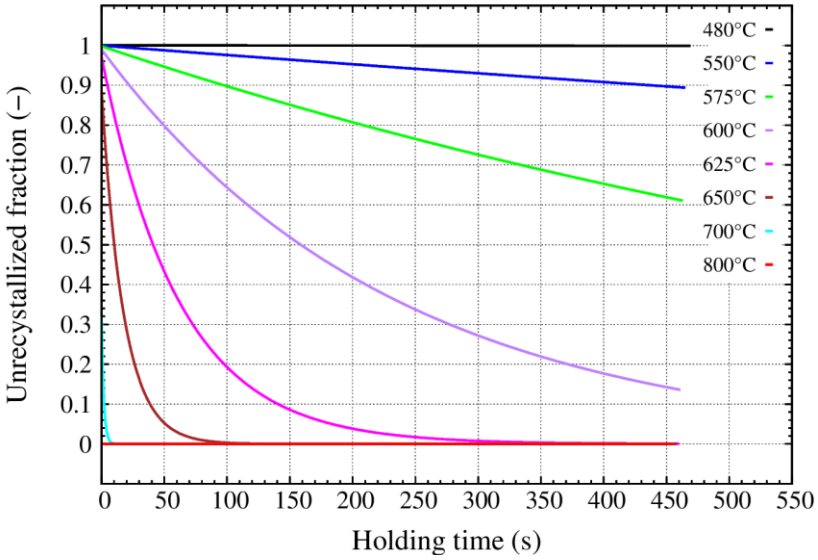

Figure 5. Isothermal hold results

For a given temperature, the unrecrystallized fraction decreases with increasing holding time. The impact of holding time is stronger when the temperature is higher. From around 575 °C the impact becomes significant. With a heating temperature of $15\ °C \cdot s^{-1}$ the materials tested at a temperature of 800 °C or more would be completely recrystallized in the heating phase preceding the carrying out of the test. 100 seconds of holding are enough to recrystallize a material at 650 °C.

Based on the kinetics parameters presented in Table 3 and Equation (5), recrystallization maps can be plotted to anticipate the recrystallization process. 2D recrystallization maps, giving the evolution of the unrecrystallized fraction as a function of temperature and time, is presented in Figure 6 for a heating rates of 1, 5, 15 and $30\ °C \cdot s^{-1}$. When the target temperature is reached a holding time is simulated. For this graph, the initial instant (0 seconds) corresponds to ambient temperature and a completely CWSR state (F=1). The temperature increase is simulated up to several target temperatures, a holding time is then applied.

The recrystallization maps obtained for Zircaloy-4 would be useful for the selection of holding time and heating rate preceding isothermal tests performed on Zircaloy-4 cladding. The maps show that in usual isothermal mechanical test at high temperature (> 600°C) the material is probably wholly recrystallized when load is applied whereas it is not during a transient where load is applied at the very beginning.

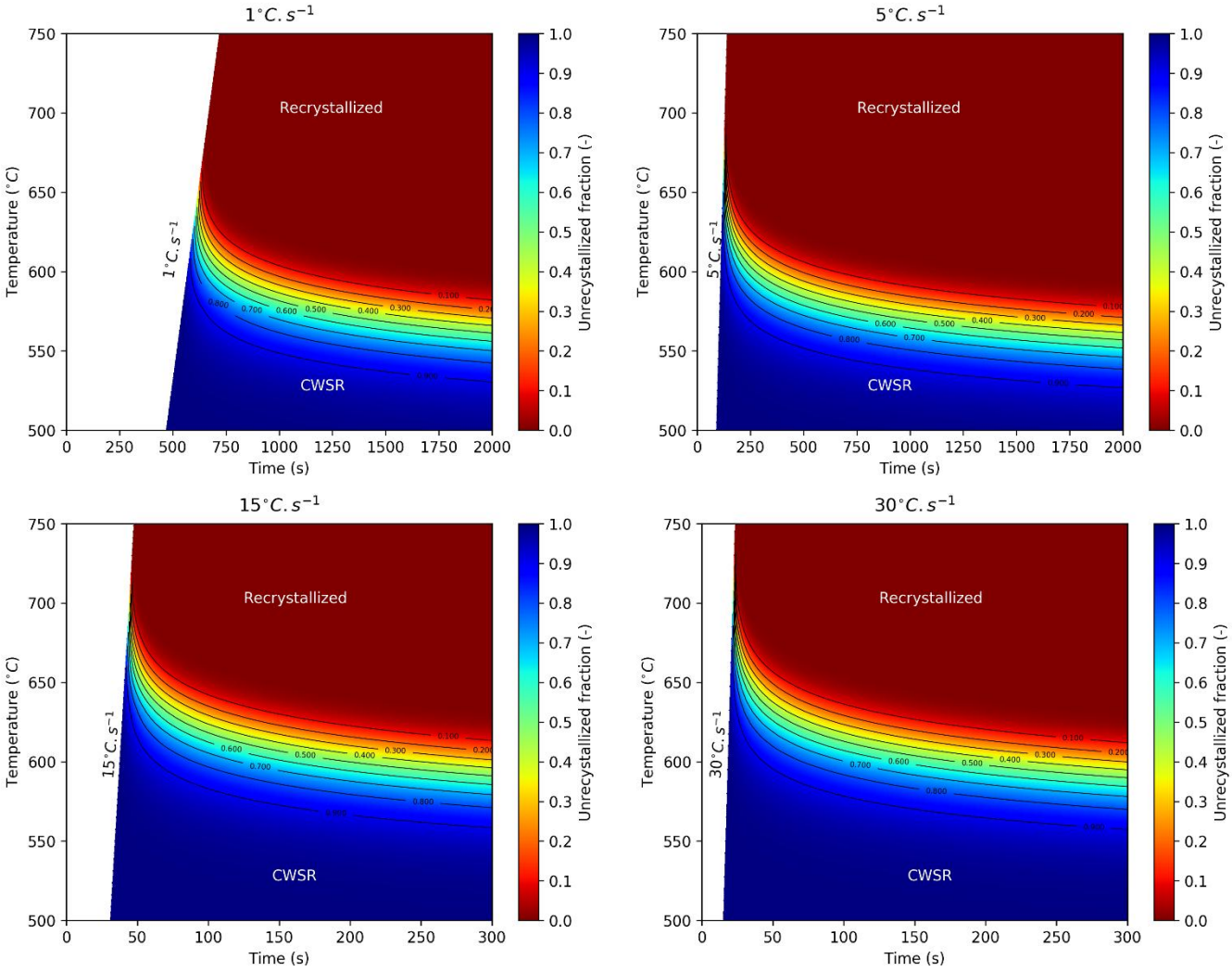

Figure 6. Diagrams of the fraction of non-recrystallized material as a function of temperature and time at $1, 5, 15$ *and* $30\ °C \cdot s^{-1}$

4. Summary and perspectives

The process of recovery-recrystallization of Zircaloy-4 cladding was evaluated during fast thermal transients. Numerous heating tests were performed with heating rates ranging from 28 to $430\ °C \cdot s^{-1}$ to study the effect of rapid thermal transients. The onset of recrystallization was found to be delayed during anisothermal heating. Recrystallization curves shift towards the high temperatures with increasing heating rates. Above $200\ °C \cdot s^{-1}$ the heating rate effect saturates, the temperature at which the transformation ends is also impacted by the heating rate.

Based on Hunt's work, a model was proposed to account for the recovery-recrystallization process. The model successfully describes recovery-recrystallization kinetics of Zircaloy-4 under isothermal and anisothermal conditions up to $430\ °C \cdot s^{-1}$.

The metallurgical state of the material plays a major role in the mechanical response of Zircaloy fuel claddings [24]. The recrystallization kinetics must always be considered when laboratory tests are performed above 500 °C.

Simple evaluation shows that the material could be recrystallized before the beginning of isothermal test, especially those at high temperature, which could lead to mechanical

properties evolution and so changes in test results are expected.
As an outlook of this work, the developed model could be integrated in numerical behavior laws to take into account the mechanical properties evolution due to recovery-recrystallization during rapid transients. These behavior laws could be dedicated to describe the thermomechanical behavior of fuel clads during accidental situations like RIA. This work could be completed by a metallurgical study to investigate and distinguish the role of recovery and recrystallization [25] during rapid thermal transients and the model could be enhanced to describe the microstructural evolutions expected during rapid transients. A coupled model for recovery, nucleation and growth of recrystallization could be developed and applied to experimental data. For irradiated materials that are the ultimate goal of this work, it is clear that annealing of irradiation defects superimposes with the recovery-recrystallization process.

5. References

[1] J. Desquines, D. A. Koss, A. T. Motta, B. Cazalis and M. Petit, "The issue of stress state during mechanical test to assess cladding performance during reactivity-initiatedaccident (RIA)," *Journal of Nuclear Materials,* vol. 412, p. 250–267, 2011.

[2] J. Papin, B. Cazalis, J. Frizonnet, J. Desquines, F. Lemoine, V. Georgenthum, F. Lamare and M. Petit, "Summary and interpretation of the CABRI REP-Na program," *Nuclear Technology,* vol. 157(3), pp. 230-250, 2007.

[3] F. Schmitz and J. Papin, "High burnup effects on fuel behaviour under accident conditions: the tests CABRI REP-Na," *Journal of Nuclear Materials,* vol. 270, pp. 55-64, 1999.

[4] T. Fuketa and H. Sasajima, "Behavior of high burnup PWR fuels with low-tin Zircaloy-4 cladding under reactivity-initiated-accident conditions," *NuclearTechnology 133(1),* pp. 50-62, 2001.

[5] T. Fuketa, F. Nagase, K. Ishijima and T. Fujishiro, "NSRR/RIA experiments with high-burnup PWR fuels," *Nuclear Safety 37(4),* pp. 328-342, 1996.

[6] S. Neogy, D. Srivastava, J. Chakravartty, G. Dey and S. Banerjee, "Microstructural Evolution in Zr-1Nb and Zr-1Nb-1Sn-0.1Fe Alloys," *Metallurgical and Materials Transactions A,* vol. 38, 2007.

[7] T. Hang, W. Xitao, G. Weijia, Z. Jun and Z. Hailong, "Recrystallization behavior of cold-rolled Zr–1Nb alloy," *Journal of Nuclear Materials,* vol. 456, pp. 321-328, 2015.

[8] D. Lee, "Recrystallization and mechanical behavior of Zircaloy-2 tubing," *Journal of Nuclear Materials,* vol. 37, pp. 159-170, 1970.

[9] M. Sauby and D. Lee, "Recovery behavior of cold-worked and quenched Zircaloy with varying oxygen content," *Journal of Nuclear Materials,* vol. 50, no. 2, pp. 175-182, 1974.

[10] N. Nagai, T. Kakuma and K. Fujita, "Texture Control of Zircaloy Tubing During Tube Reduction," ASTM International, 1982, pp. 26-38.

[11] A. A. Bauer and L. M. Lowry, "Tensile Properties and Annealing Characteristics of H. B. Robinson Spent Fuel Cladding," *Nuclear Technology,* vol. 41, no. 3, pp. 359-372, 1978.

[12] E. Steinberg, H. Weidinger and A. Schaa, "Analytical Approaches and Experimental Verification to Describe the Influence of Cold Work and Heat Treatment on the Mechanical Properties of Zircaloy Cladding Tubes," ASTM International, 1984, pp. 106-121.

[13] G. Bäro, H. Wessjohann and A. Nicoll, "On the Short-Time Recrystallization of Zircaloy-4 Above 600°C," ASTM International, 1984, pp. 200-209.

[14] P. Merle, C. Vauglin, G. Fantozzi, J. Derep and D. Charquet, "Study by Thermoelectric Power Measurements of Recovery and Recrystallization of Cold-Rolled Zircaloy-4 Sheets," ASTM International, 1987, pp. 555-576.

[15] Y.-S. Lim, H.-G. Kim and Y.-H. Jeong, "Recrystallization Behavior of Zr-xNb Alloys," *MATERIALS TRANSACTIONS,* vol. 49, no. 7, pp. 1702-1705, 2008.

[16] W. Rumball, "The effect of chromium, oxygen and microstructure on the hardness of zirconium-chromium alloys," *Journal of the Less Common Metals,* vol. 39, no. 1, pp. 35-42, 1975.

[17] A. Sarkar and J. Chakravartty, "Hot deformation behavior of Zr–1Nb alloy: Characterization by processing map," *Journal of Nuclear Materials,* vol. 440, no. 1, pp. 136-142, 2013.

[18] B. Cazalis, J. Desquines, C. Poussard, M. Petit, Y. Monerie, C. Bernaudat, P. Yvon and X. Averty, "The PROMETRA program : Fuel cladding mechanical behavior under high strain rate," *Nuclear Technology,* vol. 157, pp. 215-229, 2007.

[19] C. E. L. Hunt and E. M. Schulson, "Recrystallization of Zircaloy-4 during transient heating," *Journal of Nuclear Materials,* vol. 92, pp. 184-190, 1980.

[20] M. Gagné and E. Schulson, "The effects of annealing on cold-worked Zr3Al," *Metallurgical and Materials Transactions A-physical Metallurgy and Materials Science,* vol. 7, pp. 1775-1783, 1976.

[21] A. J. d. O. Zimmermann and A. F. PADILHA, "Rolling and recrystallization behavior of pure zirconium and zircaloy-4," *Matéria (Rio J.),* vol. 24, no. 3, 2019.

[22] J. Dunlop, Y. Bréchet, L. Legras and H. Zurob, "Modelling isothermal and non-isothermal recrystallisation kinetics: Application to Zircaloy-4," *Journal of Nuclear Materials,* vol. 366, no. 1-2, p. 178–186, 2007.

[23] H. E. Sills and R. A. Holt, "Predicting high-temperature transient deformation from microstructural models," *Zirconium in the Nuclear Industry,* vol. American Society for Testing and Materials, no. ASTM - STP 681, pp. 325-341, 1979.

[24] F. Garzarolli, R. Manzel, S. Reschke and E. Tenckhoff, "Review of Corrosion and Dimensional Behavior of Zircaloy under Water Reactor Conditions," ASTM International, 1979, pp. 91-106.

[25] J. Muntasell, J. Navarro, E. Cesari and A. Planes, "Recovery and recrystallization of zircaloy-4," *Thermochimica Acta,* vol. 87, pp. 169-176, 1985.